IEEE Photonics Journal
An IEEE Photonics Society Publication

Open Access
Invited Paper

Germanium on Silicon for Near-Infrared Light Sensing

Volume 1, Number 2, August 2009

Lorenzo Colace, Member, IEEE
Gaetano Assanto, Senior Member, IEEE

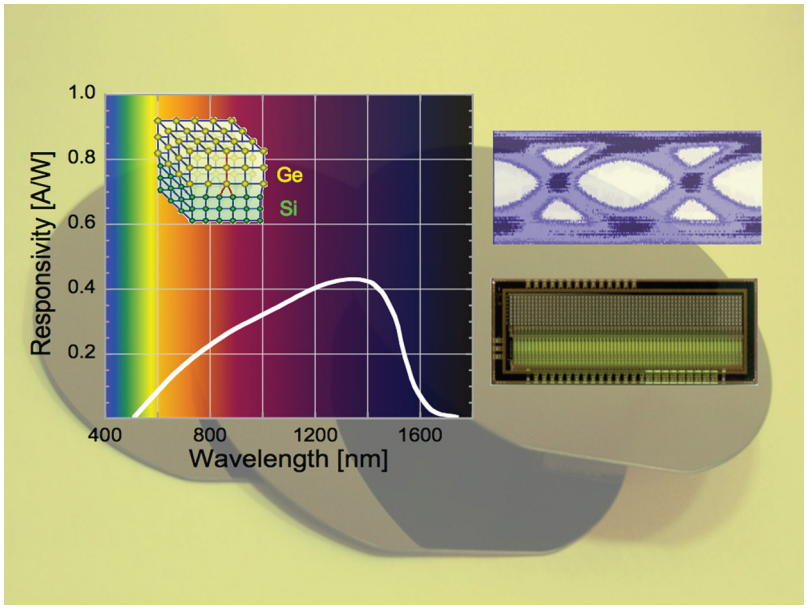

DOI: 10.1109/JPHOT.2009.2025516
1943-0655/$25.00 ©2009 IEEE

Germanium on Silicon for Near-Infrared Light Sensing

Lorenzo Colace, *Member, IEEE*, and Gaetano Assanto, *Senior Member, IEEE*

(Invited Paper)

NooEL—Nonlinear Optics and OptoElectronics Lab., University "Roma Tre," 00146 Rome, Italy

DOI: 10.1109/JPHOT.2009.2025516

Manuscript received May 15, 2009; revised June 5, 2009. First published Online June 16, 2009. Current version published July 17, 2009. Corresponding author: L. Colace (e-mail: colace@uniroma3.it).

Abstract: We review near-infrared detectors in germanium grown on silicon. We discuss *pn* and *pin* photodiodes based on Ge deposited on Si by a number of techniques, including thermal evaporation; the optical and electronic characterization of Ge-on-Si heterostructures using various approaches to minimize the density of defects; and compatibility issues with standard fabrication processes for Si electronics. We describe in greater detail the most promising devices realized by us and operating either at normal incidence or in guided-wave geometries, with applications to high-speed optical receivers, as well as image sensors.

Index Terms: Germanium, Si-based optoelectronics, photodetectors, near infrared.

1. Introduction

Wavelengths in the near infrared (NIR) are relevant in several applications, first among them optical communications with transmission windows at 0.85 (first), 1.3 (second) and 1.55 μm (third) as dictated by source availability and attenuation minima in glass fibers. Recently, wavelength division multiplexing for high-capacity links extended second and third windows to the whole interval between 1.3 and 1.6 μm. Although optical fiber communications remains the main driving force for research in NIR detectors toward high-performance optical receivers, other areas such as NIR metrology, imaging and spectroscopy have also become active fields of investigation for applications to remote sensing of the environment, monitoring of industrial processes and pollution, automotive security, biology and medicine.

Nowadays, in the area of fiber networks where the market is largely dominated by hybrid III–V semiconductor photodiodes, system performance and complexity require the development of suitable technologies for NIR optoelectronics integrated circuits able to combine optics and electronics functions in order to improve compactness, reliability, parasitic minimization and scalability while reducing the overall cost. [1] Silicon-based NIR detectors have reached a good degree of maturity, [2]–[4] particularly in Ge-on-Si structures owing to Ge absorption above 1.1 μm and its substantial compatibility with the widely diffused (and still unsurpassed) silicon technology.

In spite of the fact that a 4% lattice mismatch between Ge and Si crystals introduces a relatively large number of dislocations, [5] the epitaxial growth of pure germanium on silicon has been successfully achieved in conjunction with treatments for reducing the defect density. In the last 20 years, Ge-on-Si threading dislocation density (TDD) has been lowered from 10^8-10^9 cm^{-2} of the first direct growths [6] down to the recently achieved and remarkably low value of $5 \cdot 10^5$ cm^{-2}. [7] These treatments include compositionally graded SiGe buffers, [8] low-temperature thin Ge layers, [9] buffers combined with thermal annealing [10] and virtual substrates [11].

Ge heteroepitaxy on Si substrates is suitable for advanced NIR applications: high-performance devices, often comparable with III–V solutions, have been proposed and demonstrated. The highest cutoff frequency of 49 GHz was recently achieved by Berroth and coworkers in Ge-on-Si *pin* photodetectors fabricated by MBE with a thin Ge buffer and a Ge epilayer with TDD $= 10^8$ cm^{-2}. [12] However, the dark current density (DCD) was 100 mA/cm^2 at 1 V and the external quantum efficiency limited to 4% at 1.55 μm. Huang *et al.* reported *pn* photodiodes with thin SiGe buffer layers and thermal annealing, exhibiting a bandwidth of 8 GHz, a responsivity $R = 0.37$ A/W and DCD $= 13$ mA/cm^2 at a reverse bias of 1 V. [13] A further increase in responsivity up to $R = 0.73$ A/W with a 12 GHz bandwidth was obtained by Dosunmu and collaborators by embedding *pin* photodiodes in resonant cavities. [14] Photodiodes based on Ge lateral *pin* were operated up to 15 GHz with $R = 0.037$ A/W at 1.55 μm [15] and up to 29 GHz with $R = 0.26$ A/W at 850 nm. [16] The latter were also tested with complementary metal–oxide–semiconductor (CMOS) trans-impedance amplifiers (TIAs) and operated error free up to 19 Gb/s. Last year, a remarkable gain-bandwidth product of 340 GHz was reported in Ge-on-Si avalanche photodiodes, with DCD $= 18$ mA/cm^2. [17] To overcome the intrinsic responsivity-bandwidth limitation of normal incidence structures, a number of guided-wave detectors were investigated, including *pin* operating at 7.2 GHz with $R_w = 1.08$ A/W, [18] *pin* operating at 30 GHz with $R_w = 1.16$ A/W [19] and Ge detectors integrated on silicon on insulator (SOI) waveguides with $R_w = 0.4$ A/W at 1.55 μm and a dark current of 0.1 μA [20].

The recent scientific literature shows that Ge heteroepitaxy on Si is mature enough for high speed and responsivity, the residual density of threading dislocations being responsible for sizable dark currents. Nevertheless, the integration of Ge-on-Si technology in standard fabrication processes is still an open challenge, with only two reported examples of monolithic integration of Ge photodetectors with Si electronics. One of them was obtained by chemical vapor deposition (CVD) of Ge in a CMOS foundry; it consists of Ge-on-SOI guided-wave detectors operating at 10 Gbit/s, with 1.55 μm responsivity of 0.6 A/W and dark current of 10 μA at 1 V. [21] The detector is integrated with a front-end TIA in CMOS 0.13 μm technology. The second example is based on a low-temperature physical vapor deposition (PVD) of Ge on pre-existing Si electronics and will be described later in this work (Section 3).

Hereby we report on our recent work on Ge-on-Si NIR photodiodes where the technology for monolithic integration was simplified by minimizing its impact on foundry procedures and trading off on Ge quality. In Section 2 we will discuss Ge-on-Si optical and electrical characteristics as well as critical design issues for the minimization of process complexity and thermal budget. In Section 3 we will summarize the performance of Ge-on-Si photodiodes fabricated by us with different approaches and designed for a number of applications.

2. Optical and Electronic Properties of Ge on Si

Pure germanium is the best choice for the realization of Si-based NIR detectors because of its morphologic compatibility with the substrate and its substantial NIR absorption associated to a direct band gap. SiGe alloys have been previously proposed and employed as a route to reduce the defects density thanks to their smaller lattice mismatch with silicon. However, the indirect nature of SiGe band gap results in reduced absorption, making this approach ineffective for wavelengths above 1.3 μm. [22] Fig. 1 displays room-temperature optical absorption of bulk Ge [23] and of tensile strained Ge on Si. While the bulk semiconductor allows operation up to the Ge direct band edge around 1.55 μm, the strained epilayers benefit from strain-induced band shrinkage which, depending on its amount, shifts the cutoff toward longer wavelengths. [24] This effect is generally attributed to the tensile strain (owing to mismatch in thermal expansion of Ge and Si) generated during cooling from high temperatures (typical of Ge heteroepitaxy on Si). The absorption spectrum of strained Ge was accurately evaluated with a differential approach, preparing Ge-on-Si samples with the Ge epilayer selectively etched away from one half of the surface in order to measure and compare the powers incident on the sample, transmitted through Ge on Si, transmitted through Si, reflected from Ge on Si and reflected from Si, respectively [25].

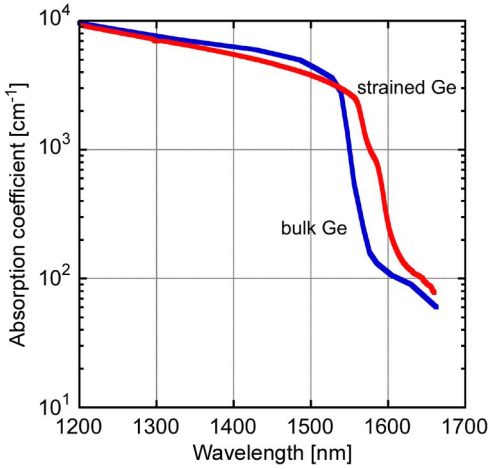

Fig. 1. Optical absorption spectra for bulk Ge and tensile strained Ge on Si.

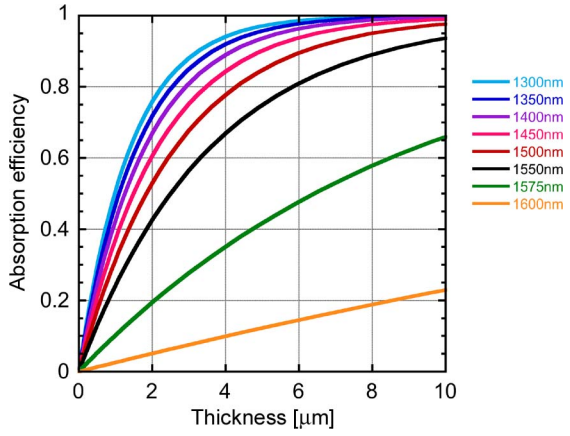

Fig. 2. Calculated absorption efficiency versus active layer thickness for strained Ge at various wavelengths (absorption data from Fig. 1).

Optical absorption has a direct impact on the detector responsivity R at normal incidence:

$$R = \frac{\lambda}{1.24}\eta_c(1-r)(1-e^{-\alpha W}) \tag{1}$$

where α is the absorption coefficient (in μm^{-1}), λ is the wavelength (in μm), η_c is the collection efficiency (i.e., the probability to collect all the photo-generated electron-hole pairs, dependent on detector type and material quality), r is the reflection coefficient from the top interface, W (in μm) is the thickness of the absorbing region; the last term in parenthesis represents the absorption efficiency, i.e., the number of photocarrier pairs per incident photon.

The absorption efficiency is graphed in Fig. 2 versus active layer thickness and various wavelengths. Clearly, since efficient detectors require a large W (order of micrometer), relaxed epilayers must be employed in spite of the inherent TDD. These defects act as recombination centers; hence, they reduce the carrier lifetime and affect both collection efficiency and DCD. Fig. 3 shows the collection efficiency we measured on *pn* photodiodes fabricated on Ge epilayers with different TDD's, with *p* and *n* Ge layers 0.2 and 0.8 μm thick, respectively. The results demonstrate that the collection efficiency can be increased with the aid of external electric fields; however, it suffers a dramatic decrease with increasing TDD.

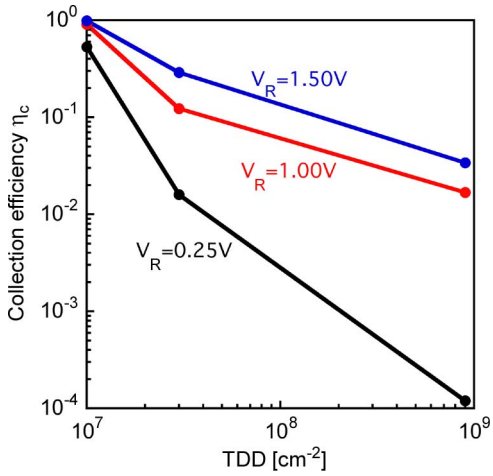

Fig. 3. Collection efficiency versus threading dislocation density for Ge/Si pn photodiodes at various reverse biases.

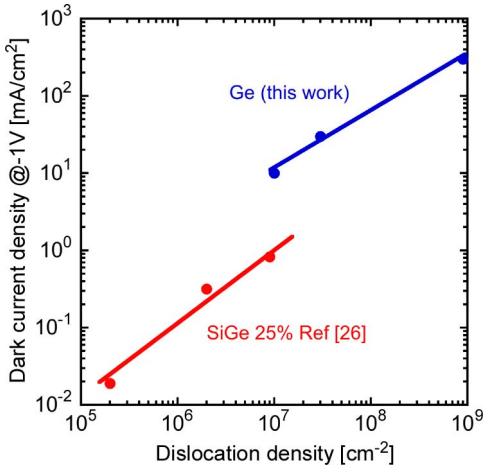

Fig. 4. DCD versus TDD for SiGe and Ge pin photodiodes.

The DCD is expected to increase with the TDD as well, since recombination in both the space charge and the neutral regions of a *pn* junction are affected by the minority carrier lifetime. Fig. 4 plots DCD of *pn* Ge diodes with various TDD, measured at a reverse bias of 1 V and shown along with results from a similar study on SiGe alloys. [26] The two sets of data, although not directly comparable because of the differences between pure Ge and SiGe, do suggest a dark current increase by one order of magnitude per decade of TDD. The most important drawback of large dark currents is the amount of shot noise, ruled by:

$$i_s = \sqrt{2q(I_{ph} + I_d)B} \tag{2}$$

with i_s being the total shot noise rms current, q the electron charge, I_{ph} the photocurrent, I_d the dark current and B the bandwidth. The minimum detectable signal in semiconductor-junction detectors is basically determined by i_s. Exceptions to the latter rule are fast photodiodes ($\approx$Gbit/s) where large dark currents can be tolerated due to a dominant current noise from high-speed TIAs (e.g., $\approx$1 μA for a 10 Gbit/s TIA). For slow communications and other low-speed applications, such as measuring and imaging, the dark current needs be minimized. To this extent, a simple and viable approach consists in scaling the device area; however, from a material standpoint, a large DCD is often a

symptom of poor reliability and linearity. Moreover, lower dark currents simplify both the design and the operation of front-end electronics [27].

From the discussion above on the role of TDD on responsivity and dark current, it is apparent that the defect density should be minimized to improve performance. Although TDD $< 10^6$ cm^{-2} have been reported, such high-quality Ge films were obtained with non-standard reactors such as ultra high vacuum CVD (UHV-CVD) [8] or molecular beam epitaxy (neither of them available in a CMOS silicon foundry), [7] complex growth schemes (thick graded buffers) and high thermal budgets (annealing). [10] In the next section we describe our work on NIR detectors fabricated with approaches all aimed at controlling the dislocation density while preserving compatibility and feasibility of integration with standard silicon processes.

3. Ge-on-Si NIR Sensing Devices

With the basic objective of optimizing the Ge epilayer quality using simple, Si-compatible and low-thermal-budget growth processes, we realized Ge-on-Si photodetectors using three different approaches: a) UHV-CVD with thin low-temperature Ge buffers, with and without thermal treatment; b) low-pressure CVD (LP-CVD) with a similar growth scheme; and c) PVD at low temperatures.

3.1. Ge-on-Si photodetectors by CVD

CVD-grown photodetectors are *pin* diodes and use a low-temperature Ge buffer to minimize TDD. Such devices were fabricated in different reactors and structures.

UHV-CVD samples were grown on silicon at a base pressure of $3 \cdot 10^{-9}$ Torr. The thin (30 nm) Ge buffer was deposited on Si at 350 °C. The buffer was meant to promote the insertion of dislocations as a mechanism for strain relaxation (i.e., as an alternative to island growth). [28] Then the reactor temperature was increased up to 600 °C and intrinsic Ge was deposited on Si. In order to further reduce the residual dislocation density, a cyclic thermal annealing (between 780 and 900 °C) was performed on samples of the series denoted by HVA. Samples denoted by HVNA were prepared without annealing to further reduce the thermal budget. The bottom p^+ contact was the high-conductivity Si substrate $(\rho = 0.008\ \Omega\text{cm})$, while the top n^+ contact was obtained by phosphorous implantation at 30 keV with a dose of $4 \cdot 10^{15}$ cm^{-2}, followed by dopant activation at 600 °C [29].

Samples denoted by LPA were fabricated by LP-CVD and the same growth sequence for the Ge buffer. However, in LPA devices a 1 μm Ge layer followed the low-temperature Ge buffer with a two-fold function: further reducing TDD and realizing the p^+ bottom contact. Therefore, in this case the entire *pin* structure consisted of Ge, whereas in the former a Ge/Si interface was involved in carrier transport. Both top n^+ and bottom p^+ contacts were in Ge and prepared by adding phosphine and diborane to GeH_4, respectively. The growth temperatures were the same as for UHV-CVD photodiodes [30].

The devices were characterized in terms of DCD, responsivity and speed of response. Fig. 5 shows typical DCD versus reverse bias, the best samples being LPA with DCD as low as $J_d = 1$ mA/cm^2 at 1 V, among the lowest values reported in Ge-on-Si *pin*. [31] Detectors HVA, with the p^+ contact in Si and without the extra buffer, exhibited larger DCD of 10 mA/cm^2, but HVNA (without annealing) showed even larger DCD, with J_d 100–200 mA/cm^2 and in agreement with the measured TDD. The three series did not exhibit any appreciable differences in responsivity. Although TDD was expected to affect the responsivity through collection efficiency, the large electric field across the intrinsic region was able to compensate for the recombination. Typical responsivities versus reverse bias are plotted in Fig. 6 for HVA samples. *pin* photodetectors with a 4 μm intrinsic region exhibited the highest responsivities $R = 0.89$ and $R = 0.75$ A/W at 1.3 and 1.55 μm, respectively. In this case the intrinsic layer was not fully depleted, thereby some external bias was needed to achieve complete carrier collection. In thinner devices $(\text{W} = 1\ \mu\text{m})$ designed for high-speed operation we measured $R = 0.2$ A/W at 1.55 μm, with peak responsivity even in short circuit. [29] Finally, we evaluated the device speed by acquiring the photoresponse to 10 Gbit/s pseudo-random bit sequences generated at $\lambda = 1.55$ μm The *pin* were reverse biased through a *tee* and directly coupled to the oscilloscope without a TIA. Fig. 7 shows typical eye diagrams for samples

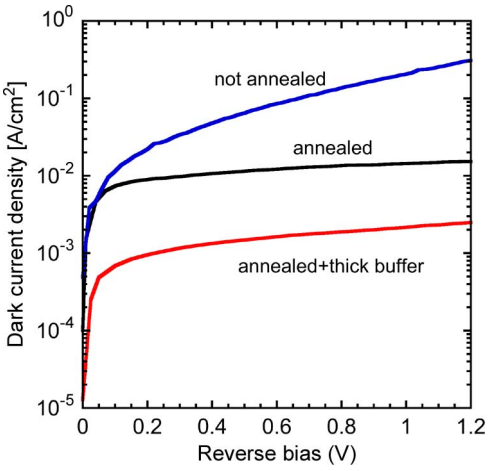

Fig. 5. DCD versus reverse bias for Ge-on-Si pin photodiodes fabricated by CVD with low-temperature Ge buffer layer.

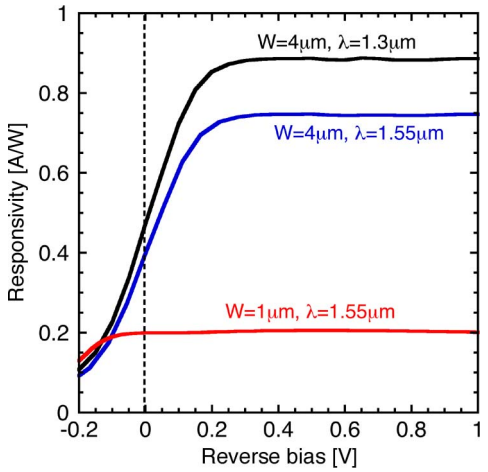

Fig. 6. Responsivity of HVA samples for various wavelengths and layer thickness.

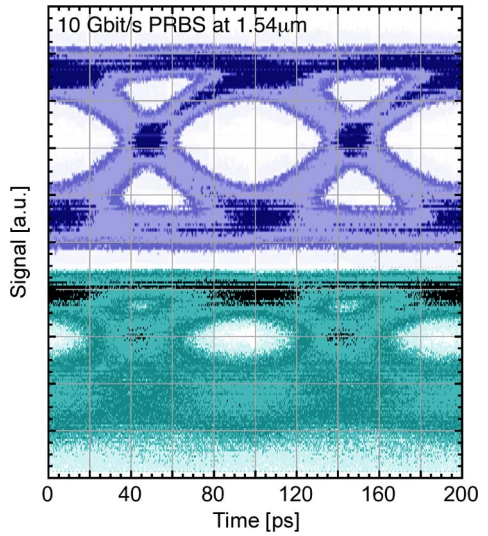

Fig. 7. 10 Gbit/s eye diagrams for (top) HVA and (bottom) LPA.

HVA and LPA, both of them with an intrinsic layer thickness $W = 1\ \mu$m and an area $A = 1.6 \cdot 10^{-5}$ cm^2. HVA devices exhibited wide open eye diagrams (comparable with the eye diagram of the source), while LPA were relatively slower due to the higher series resistance of the bottom contact. Both detector types performed extremely well at 2.5 Gbit/s (not shown) [9], [29].

The comparative analysis demonstrated the effectiveness of the low-temperature Ge buffer in yielding low-TDD Ge epilayers on Si. The growth carried at temperatures not exceeding 600 °C produced quite satisfactory detectors in terms of responsivity and speed. The associated defects affected the transport properties and gave rise to a large DCD, but the reduction in both collection efficiency and mobility was compensated by the large built-in electric field of *pin* structures. From a practical point of view, if large currents can be tolerated in ultra high-speed applications where larger noise sources (with respect to dark shot noise) are present anyway, most applications require much lower dark currents and the residual TDD has to be minimized. The latter is the benefit of introducing cyclic thermal annealing at the cost of a thermal budget with temperatures as high as 900 °C.

3.2. Ge-on-Si photodetectors by PVD

The approaches above and most of those described in literature, while able to guarantee a good Ge quality, render critical or impossible the integration with standard Si processes, especially due to the high temperatures involved. Even more critical can be the preparation of silicon surfaces, which may require temperatures above 900 °C To the latter extent, we demonstrated that vacuum evaporated Ge can be employed to fabricate NIR detectors at low (300 °C) temperatures. [32] Evaporation at ≈300 °C, with a proven tolerance up to 650 °C, provides large flexibility for its implementation in standard (e.g., CMOS) Si foundries. Using PVD we succeeded in preparing Ge-on-Si heterojunctions on CMOS integrated circuits at the very end of the Si-CMOS process. [33] The photodiodes were fabricated by PVD of germanium on silicon held at 300 °C, using grains of pure Ge (purity 99.999%) in a tungsten boat. The substrates were cleaned by diluted hydrofluoric acid and rinsed in deionized water. We report hereby on this approach to fabricate arrays of NIR image sensors integrated with CMOS electronics as well as waveguide photodetectors for integrated optics chips.

Thanks to the low-temperature PVD, Ge can be deposited subsequently to the complete fabrication of Si integrated chips, without any detrimental effects on their functionality and performance. We designed and demonstrated the operation of 8-pixel linear NIR arrays integrated with analog switches and TIA [33], linear arrays of 64 detectors with a digital output [34] and, more recently, 2-D arrays of 64 × 8 pixels. [35] The latter chips were prepared with 0.7 μm CMOS technology and included, in each row, an analog to digital converter and a digital section for control, addressing and readout. Fig. 8 shows a photograph of the whole chip, a zoomed-in portion with a few pixels and the electronics, an individual pixel and its schematic cross section. The detectors were realized by Ge PVD on the Si n-well, after opening a suitable via. Anode and cathode were obtained by the n-well contact and a p^+ diffusion (the parallel Si diode being unimportant due to its lack of sensitivity to NIR). Fig. 9 graphs the measured responsivity at 1.3 μm and the DCD versus reverse bias. While the dark current compared well with the best Ge photodetectors, the device efficiency was not equally good owing to the large defect density in the Ge layer, the latter behaving as a highly p-doped semiconductor and thereby reducing the active (depleted) region to a few nanometers, regardless of the film thickness. With these micro NIR video-cameras we acquired simple images produced by 1.55 μm light, as shown in the inset of Fig. 9.

The fundamental limitation in R associated to the large residual doping of the Ge film, with a consequent reduction of both depletion region and carrier diffusion length, can be overcome using guided-wave geometry where the absorption efficiency depends on the propagation length rather than on the detector active thickness. We fabricated Ge-on-Si photodetectors on SOI substrates, the optical guided mode being confined vertically by the SiO_2 and horizontally by the finite-width Ge mesa; it overlapped both Si and Ge layers. The photodiode was the heterojunction between the evaporated p-Ge and the n-Si overlayer of SOI, as shown in Fig. 10. [36] We realized discrete waveguide detectors (DWG) with light in-coupled through a cleaved edge and integrated devices

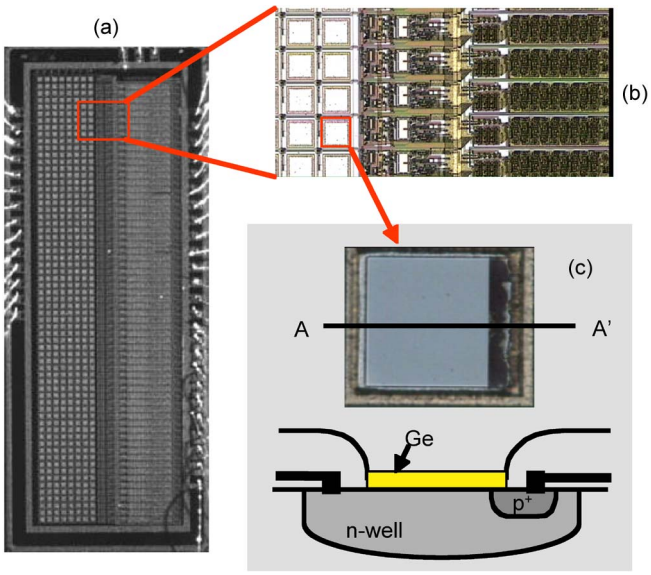

Fig. 8. (a) Photograph of the whole chip. (b) Enlargement showing a few pixels and the row electronics. (c) Photograph of a pixel and sketch of its cross section.

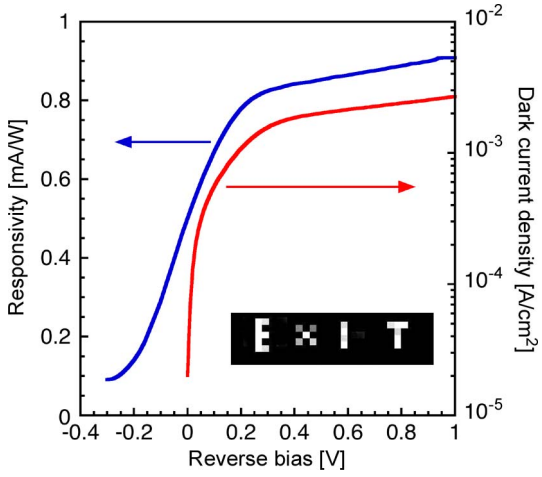

Fig. 9. DCD and NIR responsivity of a single pixel versus reverse bias. A sample image obtained with the chip at 1.3 μm is shown in the inset.

Fig. 10. Schematic cross section of a waveguide photodetector; the shaded area indicates the transverse profile of the optical guided mode.

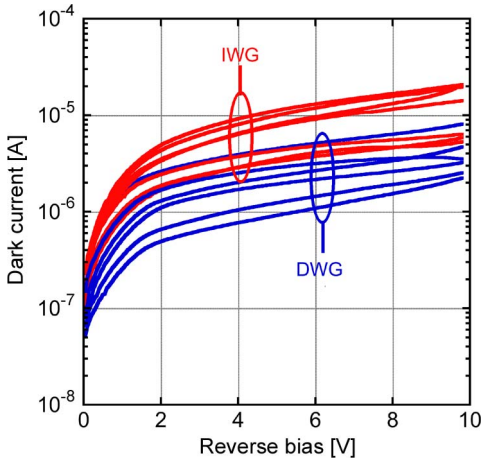

Fig. 11. DWG and IWG DCDs versus reverse bias.

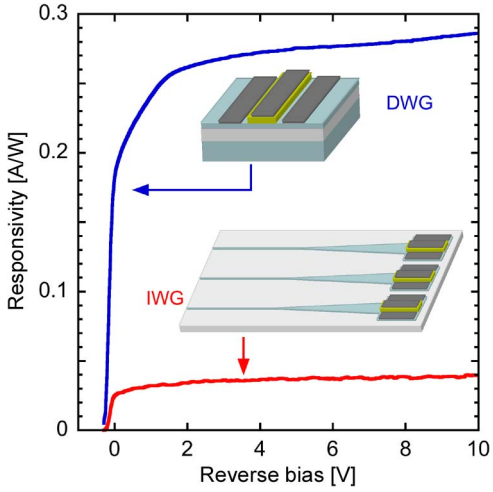

Fig. 12. DWG and IWG responsivities at 1.55 μm versus reverse bias. Sketches of both detectors are shown in the inset.

(IWG) in SOI optics chips where NIR light was in-coupled through tapered and uniform waveguides. Fig. 11 plots typical dark current densities versus reverse bias in such sensors: at 1 V reverse voltage DWG exhibited slightly lower average DCD (25 mA/cm^2) with respect to IWG (12 mA/cm^2). Substantial differences were observed in terms of responsivity, as apparent in Fig. 12: at 10 V reverse bias and 1.55 μm, DWG and IWG showed maximum responsivities $R = 0.29$ and $R = 0.04$ A/W, respectively, consistently with the inferior quality of the Ge layers in IWG realized by extra steps on a complex integrated optics chip (rather than a plain SOI as in DWG). Moreover, the doping of the Si overlayer in IWG was designed to minimize the optical losses in the passive waveguides rather than maximize photodetection. It is worth emphasizing that the DWG responsivity was $>$ 0.27 A/W at 5 V reverse bias and about 0.20 A/W in short circuit.

In any event, the low-cost, simple and Si-compatible process of these waveguide detectors make them quite promising for the realization of Si-based optoelectronics integrated circuits.

4. Conclusion

In conclusion, we have reported on our recent work on Ge-on-Si photodetectors for the NIR. We investigated Ge-on-Si optical and electrical characteristics and discussed their relationship with

device figures of merit. We have underlined the critical design issues related to minimizing the technological impact of temperature and thermal budget. Finally, we have reviewed and discussed the performance of a number of Ge-on-Si photodiodes fabricated and tested by us in high-speed optical receivers, NIR cameras and SOI optoelectronics chips.

Acknowledgment

The authors are grateful to a number of people who have contributed to various aspects of this work, including M. Balbi, V. Cencelli, R. Godfrey, L. Kimerling, H.C. Luan, G. Masini, C. Meaton, A. Perna, M. Romagnoli, L. Socci and V. Sorianello.

References

[1] R. A. Soref, "Silicon based optoelectronics," *Proc. IEEE*, vol. 81, no. 12, pp. 1687–1706, Dec. 1993.
[2] L. Colace, G. Masini, and G. Assanto, "Ge-on-Si approaches to the detection of near infrared light," *IEEE J. Quantum Electron.*, vol. 35, no. 12, pp. 1843–1852, Dec. 1999.
[3] G. Masini, L. Colace, and G. Assanto, "Si-based optoelectronics for communications," *Mater. Sci. Eng. B*, vol. 89, no. 1–3, pp. 2–9, Feb. 2002.
[4] G. Masini, L. Colace, G. Assanto, H. C. Luan, K. Wada, and L. C. Kimerling, "High performance p-i-n Ge on Si photodetectors for the near infrared: From model to demonstration," *IEEE Trans. Electron Devices*, vol. 48, no. 6, pp. 1092–1096, Jun. 2001.
[5] R. People, "Physics and applications of GeSi/Si strained-layer heterostructures," *IEEE J. Quantum Electron.*, vol. QE-22, no. 9, pp. 1696–1710, Sep. 1986.
[6] J. M. Baribeau, T. E. Jackman, D. C. Houghton, P. Maigne, and M. W. Denhoff, "Growth and characterization of SiGe and Ge epilayers on (100) Si," *J. Appl. Phys.*, vol. 63, no. 12, pp. 5738–5746, Jun. 1988.
[7] J. L. Liu, Z. Yang, and K. L. Wang, "Sb surfactant-mediated SiGe graded layers for Ge photodiodes integrated on Si," *J. Appl. Phys.*, vol. 99, no. 2, pp. 24 504–24 506, Jan. 2006.
[8] M. T. Currie, S. B. Samavedam, T. A. Langdo, C. W. Leitz, and E. A. Fitzgerald, "Controlling threading dislocation densities in Ge on Si using graded SiGe layers and chemical-mechanical polishing," *Appl. Phys. Lett.*, vol. 72, no. 14, pp. 1718–1720, Apr. 1998.
[9] L. Colace, G. Assanto, D. Fulgoni, and L. Nash, "Near-infrared p-i-n Ge-on-Si photodiodes for silicon integrated receivers," *J. Lightwave Technol.*, vol. 26, no. 13, pp. 2954–2959, Jul. 2008.
[10] H. C. Luan, D. R. Lim, K. K. Lee, K. M. Chen, J. G. Sandland, K. Wada, and L. C. Kimerling, "High-quality Ge epilayers on Si with low threading-dislocation densities," *Appl. Phys. Lett.*, vol. 75, no. 19, pp. 2011–2909, Nov. 1999.
[11] V. A. Shah, A. Dobbie, M. Myronov, D. J. F. Fulgoni, L. J. Nash, and D. R. Leadley, "Reverse graded relaxed buffers for high Ge content SiGe virtual substrates," *Appl. Phys. Lett.*, vol. 93, no. 19, pp. 192 103–192 105, Nov. 2008.
[12] S. Klinger, M. Berroth, M. Kaschel, M. Oheme, and E. Kasper, "Ge on Si p-i-n photodiodes with a 3 dB bandwidth of 49 GHz," *IEEE Photon. Technol. Lett.*, vol. 21, no. 13, pp. 920–922, Jul. 2009.
[13] Z. Huang, J. Oh, and J. C. Campbell, "Back-side-illuminated high-speed Ge photodetector fabricated on Si substrate using thin SiGe buffer layers," *Appl. Phys. Lett.*, vol. 85, no. 15, pp. 3286–3288, Oct. 2004.
[14] O. Dosunmu, D. D. Cannon, M. K. Emsley, L. C. Kimerling, and S. Umlu, "High-speed resonant cavity enhanced Ge photodetectors on reflecting Si substrates for 1550-nm operation," *IEEE Photon. Technol. Lett.*, vol. 17, no. 1, pp. 175–177, Jan. 2005.
[15] T. H. Loh, H. S. Nguyen, R. Murthy, M. B. Yu, W. Y. Loh, and G. Q. Lo, "Selective epitaxial germanium on silicon on insulator high speed photodetectors using low-temperature ultrathin SiGe buffer," *Appl. Phys. Lett.*, vol. 91, no. 7, p. 073503-5, Aug. 2007.
[16] S. J. Koester, J. D. Schaub, G. Dehlinger, and J. O. Chu, "Germanium-on-SOI infrared detectors for integrated photonic applications," *IEEE J. Sel. Topics Quantum Electron.*, vol. 12, no. 6, pp. 1489–1502, Dec. 2006.
[17] Y. Kang, H. Liu, M. Morse, M. J. Paniccia, M. Zadka, S. Litski, G. Sarid, A. Pauchard, Y. Kuo, H. Chen, W. S. Zaoui, J. E. Bowers, A. Beling, D. C. McIntosh, X. Zheng, and J. C. Campbell, "Monolithic germanium/silicon avalanche photodiodes with 340 GHz gain–bandwidth product," *Nat. Photon.*, vol. 3, no. 1, pp. 59–63, Dec. 2008.
[18] D. Ahn, C. H. Hong, J. Liu, W. Giziewicz, M. Beals, L. C. Kimerling, J. Michel, J. Chen, and X. Kartner, "High-performance, waveguide integrated Ge photodetectors," *Opt. Express*, vol. 15, no. 7, pp. 3916–3921, Mar. 2007.
[19] T. Yin, R. Cohen, M. M. Morse, G. Sarid, Y. Chetrit, D. Rubin, and M. J. Paniccia, "31 GHz Ge n-i-p waveguide photodetectors on silicon-on-insulator substrate," *Opt. Express*, vol. 15, no. 21, pp. 13 965–13 971, Oct. 2007.
[20] L. Chen, P. Dong, and M. Lipson, "High performance germanium photodetectors integrated on submicron silicon waveguides by low temperature wafer bonding," *Opt. Express*, vol. 16, no. 16, pp. 11 513–11 518, Jul. 2008.
[21] G. Masini, G. Capellini, J. Witzens, and C. Gunn, "High-speed, monolithic CMOS receivers at 1550 nm with Ge on Si waveguide photodetectors," in *Proc. 20th Ann. Meet. IEEE LEOS*, 2007, pp. 848–849.
[22] T. P. Pearsall, L. Colace, A. DiVergilio, W. Jager, D. Stenkamp, G. Theodorou, H. Presting, E. Kasper, and K. Thonke, "Spectroscopy of band-to-band optical transitions in Si-Ge alloys and superlattices," *Phys. Rev. B, Condens. Matter*, vol. 57, no. 15, pp. 9128–9140, Apr. 1998.
[23] W. C. Dash and R. Newman, "Intrinsic optical absorption in single-crystal germanium and silicon at 77 °K and 300 °K," *Phys. Rev.*, vol. 99, no. 4, pp. 1151–1155, Aug. 1955.
[24] Y. Ishikawa, K. Wada, D. D. Cannon, J. Liu, H. C. Luan, and L. C. Kimerling, "Strain-induced band gap shrinkage in Ge grown on Si substrate," *Appl. Phys. Lett.*, vol. 82, no. 13, pp. 2044–2046, Mar. 2003.

[25] V. Sorianello, A. Perna, L. Colace, G. Assanto, H. C. Luan, and L. C. Kimerling, "Near-infrared absorption of germanium thin films on silicon," *Appl. Phys. Lett.*, vol. 93, no. 11, pp. 111 115–111 117, Sep. 2008.
[26] L. M. Giovane, H. C. Luan, A. M. Agarwal, and L. C. Kimerling, "Correlation between leakage current density and threading dislocation density in SiGe p-i-n diodes grown on relaxed graded buffer layers," *Appl. Phys. Lett.*, vol. 78, no. 4, pp. 541–543, Jan. 2001.
[27] J. Gowar, *Optical Communication Systems*. New York: Pearson, 1993, pp. 501–504.
[28] L. Colace, G. Masini, G. Assanto, G. Capellini, L. Di Gaspare, E. Palange, and F. Evangelisti, "Metal–semiconductor–metal near-infrared light detector based on epitaxial Ge/Si," *Appl. Phys. Lett.*, vol. 72, no. 24, pp. 3175–3177, Jun. 1998.
[29] L. Colace, M. Balbi, G. Masini, G. Assanto, H. C. Luan, and L. C. Kimerling, "Ge on Si p-i-n photodiodes operating at 10 Gb/s," *Appl. Phys. Lett.*, vol. 88, no. 10, p. 101 111-3, Mar. 2006.
[30] L. Colace, P. Ferrara, G. Assanto, D. Fulgoni, and L. Nash, "Low dark-current germanium on silicon near-infrared detectors," *IEEE Photon. Technol. Lett.*, vol. 19, no. 22, pp. 1813–1815, Nov. 2007.
[31] J. Osmond, G. Isella, D. Chrastina, R. Kaufmann, M. Acciarri, and H. von Känel, "Ultralow dark current Ge/Si(100) photodiodes with low thermal budget," *Appl. Phys. Lett.*, vol. 94, no. 20, p. 201 106-8, May 2009.
[32] G. Masini, L. Colace, and G. Assanto, "2.5 Gb/s polycrystalline germanium-on-silicon photodetector operating from 1.3 to 1.55 μm," *Appl. Phys. Lett.*, vol. 82, no. 15, pp. 2524–2526, Apr. 2003.
[33] G. Masini, V. Cencelli, L. Colace, F. DeNotaristefani, and G. Assanto, "Monolithic integration of near-infrared Ge photodetectors with Si complementary metal-oxide-semiconductor readout electronics," *Appl. Phys. Lett.*, vol. 80, no. 18, pp. 3268–3270, May 2002.
[34] G. Masini, V. Cencelli, L. Colace, F. DeNotaristefani, and G. Assanto, "Linear array of Si/Ge heterojunction photodetectors monolithically integrated with silicon CMOS readout electronics," *IEEE J. Sel. Topics Quantum Electron.*, vol. 10, no. 4, pp. 811–815, Jul. 2004.
[35] L. Colace, G. Masini, G. Assanto, F. DeNotaristefani, and V. Cencelli, "Near-infrared camera in polycrystalline germanium integrated on complimentary-metal-oxide semiconductor electronics," *Appl. Phys. Lett.*, vol. 90, no. 1, pp. 11 103–11 105, Jan. 2007.
[36] L. Colace, G. Masini, and G. Assanto, "Guided-wave near-infrared detector in polycrystalline germanium on silicon," *Appl. Phys. Lett.*, vol. 87, no. 20, pp. 203 507–203 509, Nov. 2005.